Postinjection Transmission Scanning in Myocardial ^{18}F-FDG PET Studies Using Both Filtered Backprojection and Iterative Reconstruction

Arno P. van der Weerdt, MD[1]; Ronald Boellaard, PhD[2]; Paul Knaapen, MD[1]; Cees A. Visser, MD[1]; Adriaan A. Lammertsma, PhD[2]; and Frans C. Visser, MD[1]

[1]Department of Cardiology, Institute for Cardiovascular Research-VU, VU University Medical Center, Amsterdam, The Netherlands; and [2]PET Center, Institute for Cardiovascular Research-VU, VU University Medical Center, Amsterdam, The Netherlands

The aim of the present study was to evaluate the effect of postinjection transmission scanning (Post-Tx) on both the qualitative interpretation and the quantitative analysis of cardiac ^{18}F-FDG PET images. Furthermore, the accuracy of 2 different methods to correct for emission contamination was studied. An additional aim of this study was to compare images reconstructed with both standard filtered backprojection (FBP) and an iterative reconstruction algorithm (ordered-subset maximization expectation [OSEM]). **Methods:** Sixteen patients underwent dynamic ^{18}F-FDG imaging. Both before injection of ^{18}F-FDG and after completing the emission scan, a 10-min transmission scan was performed (Pre-Tx and Post-Tx, respectively). Images were reconstructed using both FBP and OSEM. The emission study reconstructed with Pre-Tx was considered to be the gold standard. Emission studies were also reconstructed with Post-Tx, with and without correction for emission contamination. Correction for emission contamination was performed with either transmission image segmentation (TIS) or by estimating the emission bias from the last emission frame (dwell profile [DP] method). All images were then compared by calculating ratios of ^{18}F-FDG activity between corresponding myocardial segments in each patient. Furthermore, qualitative grading of ^{18}F-FDG uptake was compared between the studies. **Results:** The mean ratio of ^{18}F-FDG activity between segments from FBP-Post and FBP-Pre was 0.78 ± 0.08. When TIS and DP were used, the mean ratios were 0.80 ± 0.07 and 0.94 ± 0.06, respectively. The use of OSEM resulted in, on average, 2% lower values for ^{18}F-FDG activity as compared with FBP. The mean normalized ^{18}F-FDG uptake was higher in FBP-Post, especially in segments with decreased ^{18}F-FDG activity. Only in the case of DP were no significant differences observed as compared with FBP-Pre. In general, qualitative analysis of the images showed that the agreement between the reconstruction methods was comparable with the reproducibility of FBP-Pre. **Conclusion:** Post-Tx for attenuation correction in cardiac ^{18}F-FDG PET scans resulted in substantial underestimation of ^{18}F-FDG activity. More accurate results were obtained with correction for emission contamination using DP. Differences in visual assessment of ^{18}F-FDG images were small. Finally, iterative reconstruction could be used as an alternative to FBP in static ^{18}F-FDG imaging of the heart.

Key Words: PET; postinjection transmission scanning; ^{18}F-FDG; iterative reconstruction

One important property of PET scanning is the possibility of accurate correction for attenuation. Attenuation correction factors can be obtained from a transmission scan that, ideally, is acquired before the tracer is administered (Pre-Tx). PET using ^{18}F-FDG is a clinically accepted and validated technique for the detection of myocardial viability (*1–6*). Most clinical studies have used qualitative interpretation of ^{18}F-FDG images or a normalized value for ^{18}F-FDG uptake to assess the presence of preserved glucose metabolism in hypoperfused segments. In such approaches, static ^{18}F-FDG PET imaging is sufficient. Static imaging is commonly performed approximately 45 min after injection of ^{18}F-FDG. This indicates that after Pre-Tx and ^{18}F-FDG injection, patients need to stay in the PET scanner for a considerable time before the actual emission scan can be performed. To shorten study protocols, postinjection transmission scanning (Post-Tx) can be performed (*7–9*). A short study protocol not only is more efficient but it also reduces motion artifacts. With Post-Tx, the transmission scan is performed after administration of the tracer and, in cardiac studies, when ^{18}F-FDG has already accumulated in the myocardium (usually 45–60 min after injection). Since high ^{18}F-FDG levels can be reached in the myocardium, Post-Tx may be accompanied by substantial emission contamination. There is only limited information, however, about the qualitative and quantitative accuracy of ^{18}F-FDG PET with Post-Tx in clinical studies (*10*). To our knowledge, no data are available concerning this issue in cardiac studies.

Correction for emission contamination in Post-Tx is possible by directly estimating emission spillover from emission data acquired just before or after the Post-Tx and subtracting this spillover from the Post-Tx (7,11) (dwell profile [DP] method) or by transmission image segmentation (TIS), in which theoretic values of attenuation coefficients (μ) are assigned to corresponding anatomic regions after segmentation of the transmission image into lung, soft tissue, and bone (12).

The aim of the present study was to evaluate the effect of Post-Tx on both the qualitative interpretation and the quantitative analysis of cardiac ^{18}F-FDG PET images. Furthermore, the accuracy of 2 different methods (DP and TIS) to correct for emission contamination was studied.

An additional aim of this study was to compare images reconstructed with both standard filtered backprojection (FBP) and an iterative reconstruction algorithm based on ordered-subset expectation maximization (OSEM). Iterative reconstruction (13,14) of PET images has been shown to improve the resolution, image contrast, and signal-to-noise ratio (15,16) compared with FBP with at least equal quantitative accuracy in some clinical studies (17–19). Moreover, OSEM algorithms have recently been implemented in standard scanner software, which may lead to more frequent use in future PET studies. Data relating to the accuracy of OSEM in cardiac PET studies, however, are still limited.

MATERIALS AND METHODS

Patients

Sixteen consecutive patients with ischemic heart disease were included in this study. All patients had impaired left ventricular function due to previous myocardial infarction and were referred for assessment of myocardial viability. They were allowed to continue their medication but intake of diuretics was delayed until after the study. Patients had a light breakfast >4 h before ^{18}F-FDG injection. None of the patients had clinical signs of decompensated heart failure. The study was approved by the Medical Ethics Committee of the VU University Medical Center and informed consent was obtained from each patient.

Clamping Procedure

All patients underwent a hyperinsulinemic, euglycemic clamp, as described by DeFronzo et al. (20), to enhance myocardial ^{18}F-FDG uptake and ensure a metabolic steady state. The clamp was started approximately 2 h before injection of ^{18}F-FDG and continued until the end of the scanning protocol. An antecubital cannula was used for infusion of insulin (human Velosulin, 100 U/mL; Novo Nordisk) and glucose (500 mL 20% glucose with 10 mL 14.9% KCl). A cannula in the contralateral arm was used to withdraw blood samples for monitoring blood glucose levels. A variable amount of IU insulin (15 times the body surface area of the patient in m^2) was added to 50 mL 0.65% NaCl. This solution was infused at a constant rate of 13 mL/h after an initial priming dose of 60 mL/h followed by 30 mL/h, both lasting for 4 min. Blood glucose levels were determined every 10 min using a GlucoTouch (Lifescan) apparatus. To maintain normoglycemia (4–6 mmol/L, 72–108 mg/dL), the glucose infusion rate was adjusted after each blood glucose measurement, when needed.

Preparation of ^{18}F-FDG

^{18}F-FDG was synthesized by the BV Cyclotron VU (Amsterdam, The Netherlands) according to a modified method previously described by Hamacher et al. (21), using Nuclear Interface equipment. The radiochemical purity was >97%.

Scanning Protocol

All scans were performed in 2-dimensional mode, using an ECAT EXACT HR+ (Siemens/CTI) (22,23). This scanner acquires 63 planes of data over an axial field of view of 15 cm.

A 10-min transmission scan, using rotating ^{68}Ge line sources together with sinogram windowing, was performed after a short transmission scan for patient positioning. Subsequently, ^{18}F-FDG (370 MBq dissolved in 5 mL saline) was injected intravenously (followed by a 47-mL saline flush at a rate of 2 mL/s). A dynamic scan was performed consisting of 39 frames with variable frame length for a total duration of 60 min. Immediately after obtaining the dynamic scan, a second 10-min transmission scan was performed.

Emission data were corrected for physical decay of ^{18}F and for dead time, scatter, and randoms. The last 3 frames of the dynamic scan were summed (i.e., 45–60 min after injection) to create a single-frame emission sinogram with high-count statistics. Reconstructions of this emission sinogram were performed using both FBP with a Hanning filter at 0.5 of the Nyquist frequency and OSEM (CTI version 7.1.1) with 2 iterations of 12 subsets. OSEM images underwent 5-mm full width at half maximum (FWHM) gaussian postsmoothing to obtain a transaxial spatial resolution of 7-mm FWHM, equal to that of FBP images (18). Attenuation correction was applied using 4 different transmission scans: (a) Pre-Tx, (b) Post-Tx, (c) Post-Tx corrected for emission contamination using TIS, and (d) Post-Tx corrected for emission contamination using DP.

In this way, 8 different images (FBP-Pre, FBP-Post, FBP-PostTIS, FBP-PostDP, OSEM-Pre, OSEM-Post, OSEM-PostTIS, OSEM-PostDP) were generated from the single-frame emission sinogram for each patient.

Correction Methods for Post-Tx

TIS implies the use of theoretic μ-values for segmented anatomic regions (12). The μ-values used in the present study were 0.028, 0.095, and 0.107 cm^{-1} for lung, soft tissue, and bone, respectively. Combination with the original (measured) μ-values was performed in a weighted fashion. Weighting factors were 0.4 (lung), 0.85 (soft tissue), and 0.7 (bone).

Another correction method, based on a DP, has been described elsewhere (11). In short, this method describes the spillover fraction of emission counts into the transmission scan per line of response. The transmission scan can be corrected for emission contamination using Corrected Post-Tx = Post-Tx − Ex × DP × CF, where Ex = emission scan, DP = dwell profile, and CF = overall correction factor, which includes corrections for decay, frame length, and differences in normalization between emission and transmission data.

Data Analysis

Data were transferred to a SUN workstation (SUN Microsystems, Inc.) and were analyzed using Siemens/CTI software. Transaxial images of the left ventricle were reoriented according to the anatomic axis of the heart and subsequently displayed as short-axis slices. For each study, reslicing was first performed with FBP-Pre. The same reslicing parameters were automatically applied to the

remaining 7 transaxial images. Regions of interest (ROIs) were defined manually on each slice of the FBP-Pre short-axis image and copied to the remaining 7 short-axis images, to ensure equal ROI definition on each reconstruction. At the basal and distal levels of the left ventricle, these ROIs divided each short-axis slice into 6 regions. At the apex, 1 ROI was defined on each short-axis slice. Corresponding ROIs from a variable number of slices were grouped in each patient to compose 13 volumes of interest, representing 13 myocardial segments (6 basal, 6 distal, and 1 apex). For each segment, the mean ^{18}F-FDG activity was calculated.

All images were compared with FBP-Pre by calculating ratios of ^{18}F-FDG activity between the corresponding segments in each patient. Furthermore, for each image, every segment was normalized to the segment with the highest mean activity. Normalized data of all images were compared with those of FBP-Pre.

For qualitative analysis, all images were graded, according to the 13-segment model described above, by 2 experienced observers on a 4-point scale from 1 to 4: 1 = normal tracer uptake (>75%), 2 = mildly reduced tracer uptake (50%−75%), 3 = moderately reduced tracer uptake (25%–50%), and 4 = severely reduced or absent tracer uptake (<25%). Differences were resolved by consensus. The consensus gradings of FBP-Pre were repeated afterward to assess reproducibility. Both interobserver agreement and consensus gradings were compared between the 8 different reconstruction methods.

Statistical Analysis

All data are expressed as mean ± SD. Statistical analyses were performed using the 2-tailed paired t test and least-squares regression analysis. Interobserver agreement and agreement between individual reconstruction methods were assessed using κ-statistics.

For the normalized ^{18}F-FDG uptake, the limits of agreement were assessed by means of the analysis described by Bland and Altman (24). $P < 0.05$ was considered statistically significant.

RESULTS

Sixteen patients (11 male, 5 female) with a mean age of 63 ± 12 y were studied. Four had a history of diabetes mellitus. For each patient, 8 different images were reconstructed, resulting in a total of 128 myocardial images. Each image was divided into 13 myocardial segments. Consequently, a total of 1,664 segments were analyzed

Quantitative Analysis

^{18}F-FDG activity in the myocardial segments of FBP-Pre was 38.9 ± 17.4 kBq/mL and ranged from 6.9 to 83.8 kBq/mL. The good correlation between FBP-Pre and FBP-Post, both with and without correction for emission contamination, is shown in Figures 1A–1C. FBP-Pre and OSEM-Pre had an extremely good correlation (Fig. 1D).

The mean ratio of segmental ^{18}F-FDG activity of FBP-Post/FBP-Pre was 0.78 ± 0.08 (Table 1). Figure 2A shows this ratio as a function of the level of activity in FBP-Pre ($r^2 = 0.29$, $P < 0.001$). When TIS was used for correction of emission contamination, the mean ratio of FBP-PostTIS/FBP-Pre was 0.80 ± 0.07. Correlation with the level of activity in FBP-Pre was considerable weaker ($r^2 = 0.11$, $P < 0.001$; Fig. 2B). The mean ratio was 0.94 ± 0.06 when

DP was used and no correlation with the level of activity in FBP-Pre was found (Fig. 2C).

Comparable results were observed with iterative reconstruction, when OSEM-Pre was used as reference (Table 1). These ratios could also be correlated with the level of activity in OSEM-Pre (OSEM-Post: $r^2 = 0.33$, $P < 0.001$; OSEM-PostTIS: $r^2 = 0.10$, $P < 0.001$; OSEM-PostDP: $P =$ not significant [NS]).

The use of OSEM resulted in, on average, 2% lower values for ^{18}F-FDG activity as compared with FBP (Table 1). No correlation with the level of activity in FBP-Pre was found (Fig. 2D).

When segmental ^{18}F-FDG activity was expressed as a percentage of the highest activity, the mean normalized ^{18}F-FDG uptake was 75% ± 21% and was almost equal between all reconstruction methods. For the 30 segments with normalized ^{18}F-FDG activity of <50%, the mean value in FBP-Pre was 35% ± 8%. The corresponding segments, however, in both FBP-Post and FBP-PostTIS demonstrated a higher mean value (Table 2). In FBP-PostDP, no statistical significant difference was observed. In OSEM-Pre, the mean value was slightly lower.

For the 48 segments with normalized ^{18}F-FDG activity between 50% and 75%, FBP-Pre resulted in a mean value of 63% ± 7%. Again, corresponding segments in both FBP-Post and FBP-PostTIS yielded higher values (Table 2). The mean normalized ^{18}F-FDG activity in segments from FBP-PostDP did not differ significantly. In OSEM-Pre, the mean value was again slightly lower.

For the 130 segments with normalized ^{18}F-FDG activity > 75%, the mean value was 89% ± 8% with no significant differences between all reconstruction methods (Table 2).

Limits of agreement of the normalized segmental ^{18}F-FDG activity in FBP-Pre and the other images are shown in Figure 3. Using Post-Tx for attenuation correction (Figs. 3A–3C), the highest agreement with FBP-Pre is achieved by FBP-PostDP (Fig. 3C). Almost identical results were observed with the iterative reconstructed images and OSEM-Pre as reference (data not shown).

Qualitative Analysis

Thirteen hundred fifteen of 1,664 segments (79%) were scored similar by both observers (κ = 0.69). Interobserver agreement was comparable between the images from the 8 reconstruction methods and ranged from 77% to 82% ($P =$ NS compared with FBP-Pre). Reproducibility of the consensus grading of FBP-Pre was 88% (κ = 0.83).

Of the 208 segments in FBP-Pre (16 patients × 13 segments), by consensus, 80, 73, 41, and 14 segments were graded 1, 2, 3, and 4, respectively. From these consensus gradings, it appeared that most reconstruction methods resulted in a comparable agreement with FBP-Pre as the reproducibility of FBP-Pre itself (Table 3). Only for OSEM-PostTIS was agreement lower.
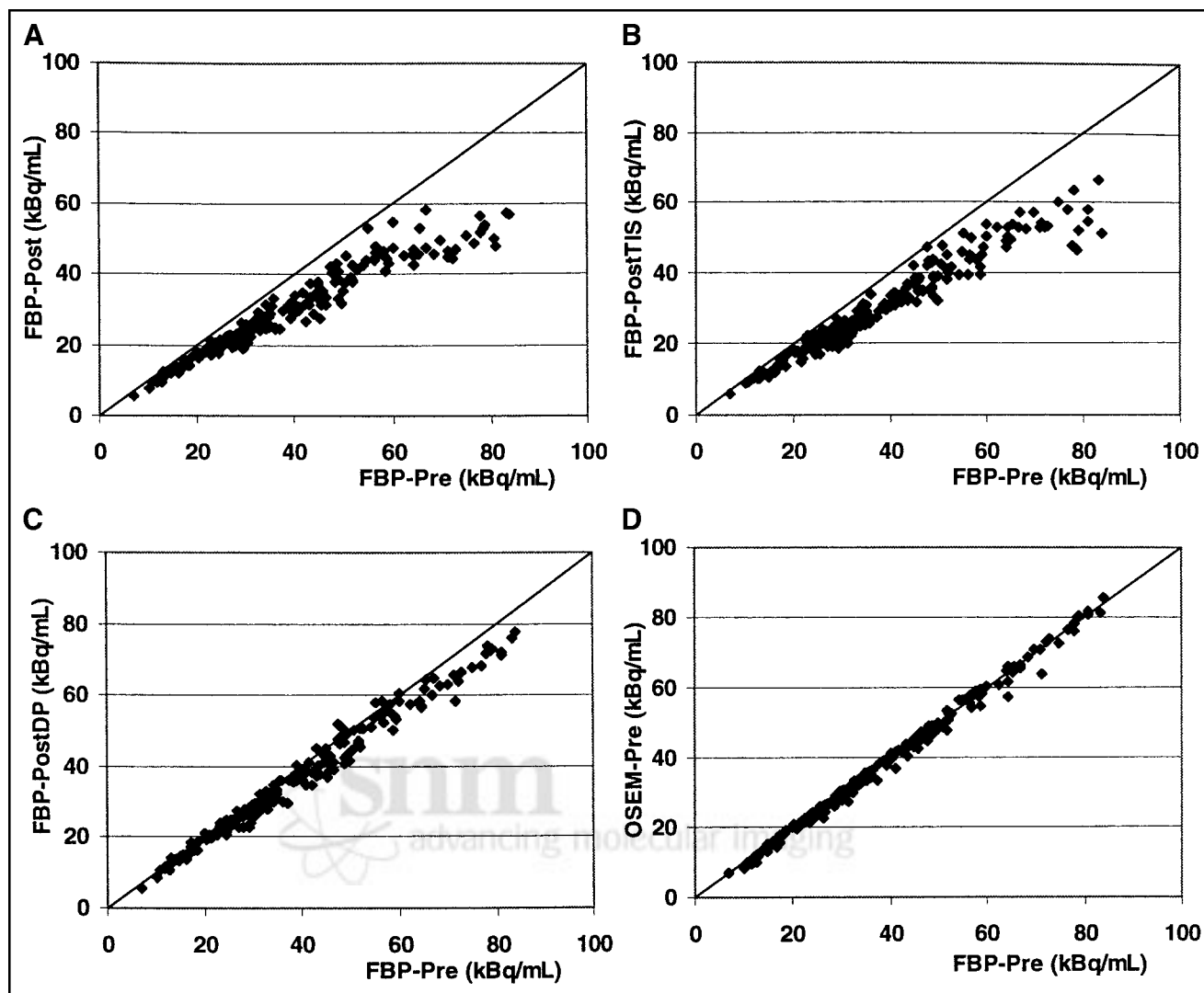
FIGURE 1. Scatter plots of the correlation between FBP-Pre and FBP-Post (A), FBP-Pre and FBP-PostTIS (B), FBP-Pre and FBP-PostDP (C), and FBP-Pre and OSEM-Pre (D). R^2 = 0.94, 0.94, 0.98, and 0.99, respectively. The solid line in the figures represents the line of unity.

Almost identical results were obtained when OSEM-Post, OSEM-PostTIS, and OSEM-PostDP were compared using OSEM-Pre as reference (agreement: 86%, 82%, and 86%, respectively).

TABLE 1
Mean Ratio of ^{18}F-FDG Activity

Image reconstruction	Ratio ± SD	P
FBP-Pre as reference		
FBP-Post	0.78 ± 0.08	<0.001
FBP-PostTIS	0.80 ± 0.07	<0.001
FBP-PostDP	0.94 ± 0.06	<0.001
OSEM-Pre	0.98 ± 0.04	<0.001
OSEM-Pre as reference		
OSEM-Post	0.80 ± 0.08	<0.001
OSEM-PostTIS	0.79 ± 0.08	<0.001
OSEM-PostDP	0.94 ± 0.06	<0.001

DISCUSSION

Although an attractive and frequently practiced procedure, there is only limited information about the qualitative and quantitative accuracy of ^{18}F-FDG PET with Post-Tx in clinical studies (10). With Post-Tx, the transmission scan is performed after the tracer is administered and, in cardiac studies, when ^{18}F-FDG has already accumulated in the myocardium. Especially during glucose loading—or even more pronounced, euglycemic hyperinsulinemic clamping—^{18}F-FDG reaches high activity levels in the myocardium. Post-Tx may, therefore, be accompanied by substantial emission contamination.

In this study, it was demonstrated that the emission contamination in PostTx resulted in approximately 20% lower values of estimated ^{18}F-FDG activity in the emission image, and this underestimation could be correlated with the local concentration. Although TIS is appealing with respect to a
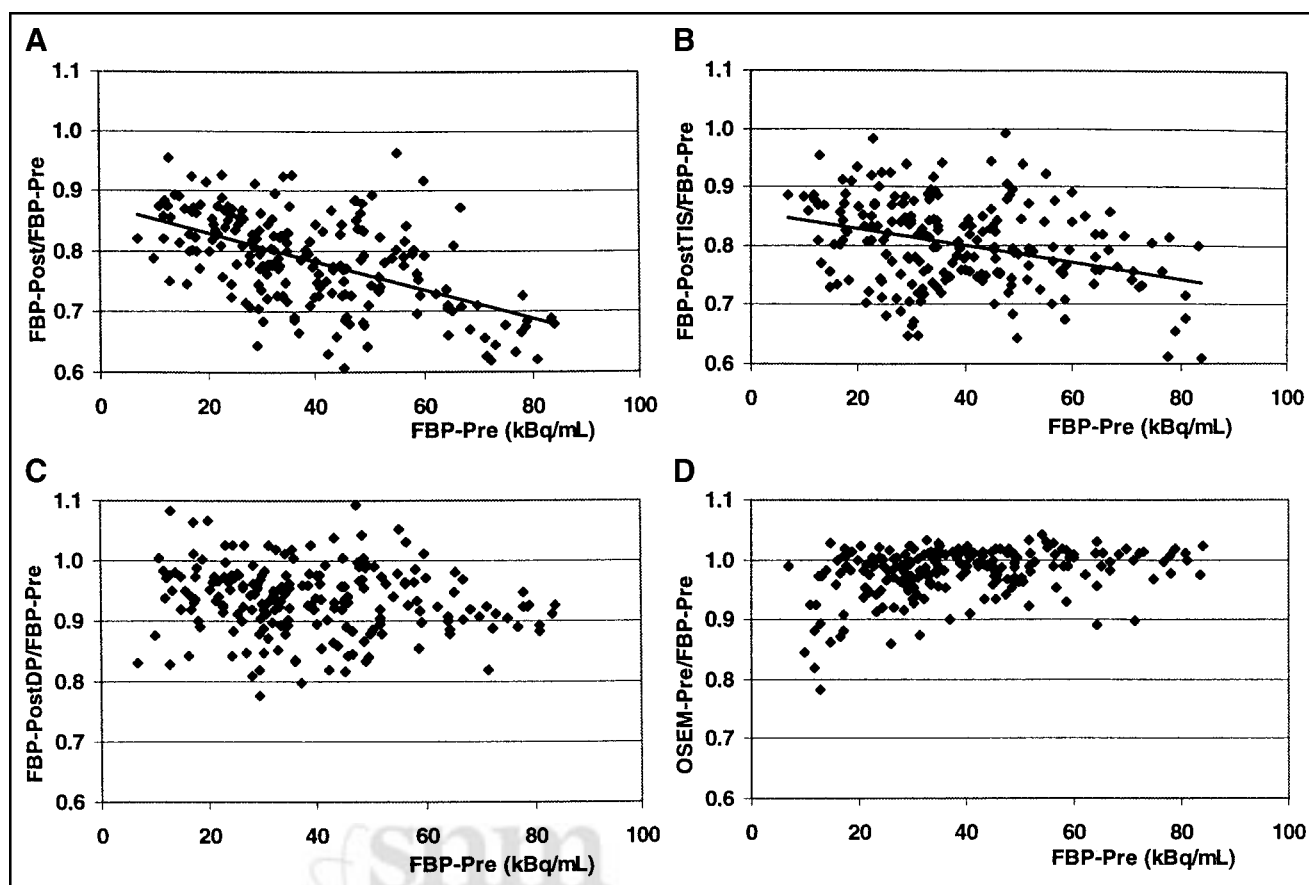
FIGURE 2. Mean ratio of ^{18}F-FDG activity between corresponding segments from FBP-Post (A), FBP-PostTIS (B), FBP-PostDP (C), and OSEM-Pre (D) and those of FBP-Pre.

shorter acquisition time together with noise reduction in the transmission image, correction for emission contamination with TIS appeared to be quantitatively inadequate. Xu et al. (12) reported accurate measurements using TIS as long as the activity concentration was <13 kBq/mL. In the present study, however, the mean ^{18}F-FDG activity in the myocardial segments was almost 40 kBq/mL. Knuuti et al. (25) reported comparable values for segmental ^{18}F-FDG activity concentration during hyperinsulinemic clamping. Although a glucose loading procedure will result in about 20% lower ^{18}F-FDG activity concentration as compared with hyperinsulinemic clamping (25), it may still be too high to allow for accurate correction of emission contamination with TIS.

When data from the last emission frame were used to correct for emission contamination in PostTx, values of ^{18}F-FDG activity were, on average, 6% lower than PreTx, representing a small undercorrection. This undercorrection might be caused by (a) a small underestimation of the dwell profile values, (b) small inaccuracies within the normalization for inhomogeneous (patient) activity distributions, or (c) redistribution of activity during the time interval between emission and transmission acquisition. Although emission subtraction increases statistical noise, this method did not result in a higher variation in the results compared with images without such correction.

TABLE 2
Mean Normalized ^{18}F-FDG Activity

Image reconstruction	Mean ± SD (%)	P
Segments with <50% ^{18}F-FDG uptake		
(n = 30)		
FBP-Pre	35 ± 8	
FBP-Post	39 ± 9	<0.001
FBP-PostTIS	38 ± 9	<0.001
FBP-PostDP	36 ± 8	NS
OSEM-Pre	34 ± 8	<0.001
Segments with 50%–75% ^{18}F-FDG uptake		
(n = 48)		
FBP-Pre	63 ± 7	
FBP-Post	67 ± 8	<0.001
FBP-PostTIS	65 ± 7	0.002
FBP-PostDP	64 ± 8	NS
OSEM-Pre	62 ± 8	0.014
Segments with >75% ^{18}F-FDG uptake		
(n = 130)		
FBP-Pre	89 ± 8	
FBP-Post	89 ± 8	NS
FBP-PostTIS	89 ± 8	NS
FBP-PostDP	89 ± 8	NS
OSEM-Pre	88 ± 8	NS

NS = not significant.
Differences in mean normalized ^{18}F-FDG uptake between reconstruction methods and FBP-Pre as reference image.
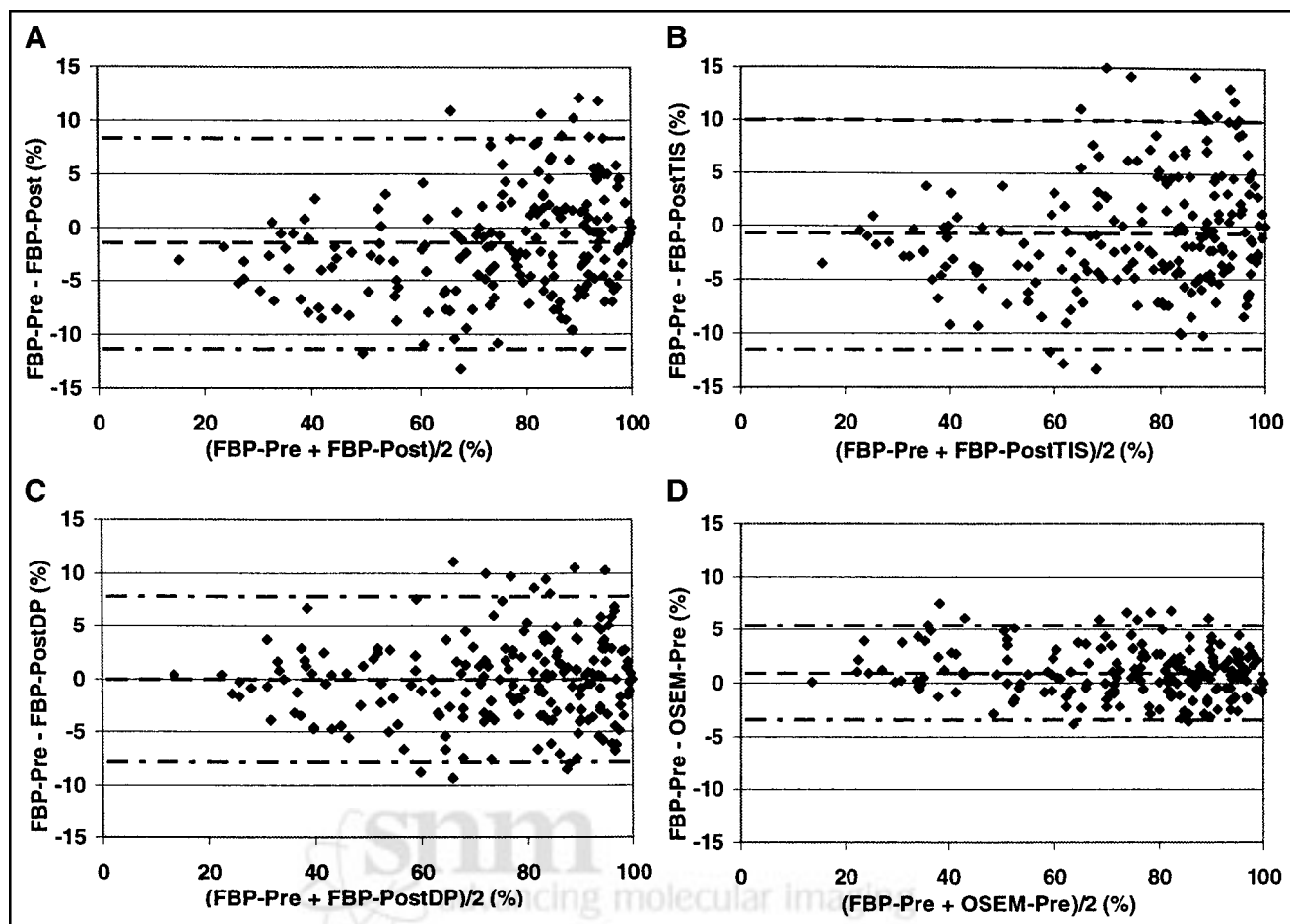
FIGURE 3. Limits of agreement for normalized segmental ^{18}F-FDG uptake in FBP-Pre and FBP-Post (A), FBP-PostTIS (B), FBP-PostDP (C), and OSEM-Pre (D). Horizontal lines represent the mean difference and mean $\pm$ 2 SD. (A) Mean = -1%; 2 SD = 10%. (B) Mean = -1%; 2 SD = 11%. (C) Mean = 0%; 2 SD = 8%. (D) Mean = 1%; 2 SD = 4%.

Since it is common practice in cardiac studies to use data of ^{18}F-FDG uptake normalized to the segment with highest tracer uptake, the effect of these quantitative differences was also evaluated using a normalized dataset. FBP-Post appeared to overestimate ^{18}F-FDG uptake especially in segments with low ^{18}F-FDG activity. For example, segments with normalized ^{18}F-FDG activity of <50% were, on average, 4% overestimated (a relative overestimation of 11%). In contrast, no significant differences were observed between all reconstruction methods in segments with normalized ^{18}F-FDG activity of >75%. Overestimation of ^{18}F-FDG activity in segments with normalized activity up to 75% was also observed in FBP-PostTIS. In contrast, with FBP-PostDP, no difference was observed compared with FBP-Pre. Correction for emission contamination, thus, results in more accurate data only when DP is used. The observed differences in ^{18}F-FDG activity in the normalized dataset, however, are rather small and are unlikely to influence clinical decision making. Nevertheless, as data for a DP correction will always be available, it seems good practice to perform such a correction on a routine basis.

TABLE 3
Agreement Compared with FBP-Pre

Analysis	Image reconstruction						
	FBP-Post	FBP-PostTIS	FBP-PostDP	OSEM-Pre	OSEM-Post	OSEM-PostTIS	OSEM-PostDP
Agreement (segmental) (%)	86	84	85	88	83	77*	85
κ	0.80	0.76	0.78	0.82	0.75	0.66	0.78

*P = 0.003, when compared with the agreement in the reproducibility study of FBP-Pre.

All images were of good quality, and qualitative analysis of the images showed no difference in interobserver agreement between reconstruction methods. In general, the agreement between the reconstruction methods was comparable with reproducibility of FBP-Pre itself.

Iterative reconstruction has proven to be a robust alternative to FBP in static ^{18}F-FDG imaging of the heart. Both quantitative and qualitative data closely resembled the corresponding FBP data. Although images looked smoother than with FBP, a real advantage of iterative reconstruction was not observed in this patient population undergoing hyperinsulinemic euglycemic clamping, where FBP also resulted in high-quality images

Patient movement is a potential confounder in this study comparing Pre-Tx and Post-Tx for attenuation correction, as the preinjection transmission scan would not be the gold standard in this situation. Patient movement, however, was minimized by using arm supports and strips around the body of the patient. Furthermore, pre- and postinjection transmission scans were compared to assess the magnitude of patient movement in each study. Using this analysis, for the present series of patients, these movements were considered to be small. Finally, with large myocardial ROIs, the effects of movement will be less.

CONCLUSION

Post-Tx for attenuation correction in cardiac ^{18}F-FDG PET scans results in substantial underestimation of ^{18}F-FDG activity. The small effects in normalized datasets will probably have only minor consequences in clinical decision making. More accurate results, however, are obtained with correction for emission contamination using DP, and there is no reason not to implement this method on a routine basis. No differences are observed in qualitative interpretation of ^{18}F-FDG images. Finally, iterative reconstruction can be used as an alternative to FBP in static ^{18}F-FDG imaging of the heart.

REFERENCES

1. Marshall RC, Tillisch JH, Phelps ME, et al. Identification and differentiation of resting myocardial ischemia and infarction in man with positron computed tomography, ^{18}F-labeled fluorodeoxyglucose and N-13 ammonia. *Circulation.* 1983;67:766–778.
2. Tillisch J, Brunken R, Marshall R, et al. Reversibility of cardiac wall-motion abnormalities predicted by positron tomography. *N Engl J Med.* 1986;314:884–888.
3. Tamaki N, Yonekura Y, Yamashita K, et al. Positron emission tomography using fluorine-18 deoxyglucose in evaluation of coronary artery bypass grafting. *Am J Cardiol.* 1989;64:860–865.
4. Schwaiger M, Brunken R, Grover-McKay M, et al. Regional myocardial metabolism in patients with acute myocardial infarction assessed by positron emission tomography. *J Am Coll Cardiol.* 1986;8:800–808.
5. Marwick TH, MacIntyre WJ, Lafont A, Nemec JJ, Salcedo EE. Metabolic responses of hibernating and infarcted myocardium to revascularization: a follow-up study of regional perfusion, function, and metabolism. *Circulation.* 1992;85:1347–1353.
6. Gropler RJ, Geltman EM, Sampathkumaran K, et al. Comparison of carbon-11-acetate with fluorine-18-fluorodeoxyglucose for delineating viable myocardium by positron emission tomography. *J Am Coll Cardiol.* 1993;22:1587–1597.
7. Carson RE, Daube-Witherspoon ME, Green MV. A method for postinjection PET transmission measurements with a rotating source. *J Nucl Med.* 1988;29:1558–1567.
8. Daube-Witherspoon ME, Carson RE, Green MV. Post-injection transmission attenuation measurements for PET. *IEEE Trans Nucl Sci.* 1988;35:757–761.
9. Ranger NT, Thompson CJ, Evans AC. The application of a masked orbiting transmission source for attenuation correction in PET. *J Nucl Med.* 1989;30:1056–1068.
10. Hooper PK, Meikle SR, Eberl S, Fulham MJ. Validation of post-injection transmission measurements for attenuation correction in neurological FDG-PET studies. *J Nucl Med.* 1996;37:128–136.
11. Luk WK, Digby WD, Jones WF, Casey ME. An analysis of correction methods for emission contamination in PET post-injection transmission measurement. *IEEE Trans Nucl Sci.* 2001;42:2303–2308.
12. Xu M, Luk WK, Cutler PD, Digby WM. Local threshold for segmented attenuation correction of PET imaging of the thorax. *IEEE Trans Nucl Sci.* 1994;41:1532–1537.
13. Shepp LA, Vardi Y. Maximum likelihood reconstruction for emission tomography. *IEEE Trans Med Imaging.* 1982;1:113–122.
14. Hudson HM, Larkin RS. Accelerated image reconstruction using ordered subsets of projection data. *IEEE Trans Med Imaging.* 1994;13:601–609.
15. Miller TR, Wallis JW. Clinically important characteristics of maximum-likelihood reconstruction. *J Nucl Med.* 1992;33:1678–1684.
16. Riddell C, Carson RE, Carrasquillo JA, et al. Noise reduction in oncology FDG PET images by iterative reconstruction: a quantitative assessment. *J Nucl Med.* 2001;42:1316–1323.
17. Katoh C, Ruotsalainen U, Laine H, et al. Iterative reconstruction based on median root prior in quantification of myocardial blood flow and oxygen metabolism. *J Nucl Med.* 1999;40:862–867.
18. Boellaard R, van Lingen A, Lammertsma AA. Experimental and clinical evaluation of iterative reconstruction (OSEM) in dynamic PET: quantitative characteristics and effects on kinetic modeling. *J Nucl Med.* 2001;42:808–817.
19. Lonneux M, Borbath I, Bol A, et al. Attenuation correction in whole-body FDG oncological studies: the role of statistical reconstruction. *Eur J Nucl Med.* 1999;26:591–598.
20. DeFronzo RA, Tobin JD, Andres R. Glucose clamp technique: a method for quantifying insulin secretion and resistance. *Am J Physiol.* 1979;237:E214–E223.
21. Hamacher K, Coenen HH, Stocklin G. Efficient stereospecific synthesis of no-carrier-added 2-[^{18}F]-fluoro-2-deoxy-D-glucose using aminopolyether supported nucleophilic substitution. *J Nucl Med.* 1986;27:235–238.
22. Adam LE, Zaers J, Ostertag H, Trojan H, Bellemann ME, Brix G. Performance evaluation of the whole-body PET scanner ECAT EXACT HR+ following the IEC standard. *IEEE Trans Nucl Sci.* 1997;44:1172–1179.
23. Brix G, Zaers J, Adam LE, et al. Performance evaluation of whole-body PET scanner using the NEMA protocol. *J Nucl Med.* 1997;38:1614–1623.
24. Bland JM, Altman DG. Statistical methods for assessing agreement between two methods of clinical measurement. *Lancet.* 1986;1:307–310.
25. Knuuti MJ, Nuutila P, Ruotsalainen U, et al. Euglycemic hyperinsulinemic clamp and oral glucose load in stimulating myocardial glucose utilization during positron emission tomography. *J Nucl Med.* 1992;33:1255–1262.

The Journal of NUCLEAR MEDICINE

Postinjection Transmission Scanning in Myocardial ^{18}F-FDG PET Studies Using Both Filtered Backprojection and Iterative Reconstruction

Arno P. van der Weerdt, Ronald Boellaard, Paul Knaapen, Cees A. Visser, Adriaan A. Lammertsma and Frans C. Visser

This article and updated information are available at:
http://jnm.snmjournals.org/content/45/2/169

Information about reproducing figures, tables, or other portions of this article can be found online at:
http://jnm.snmjournals.org/site/misc/permission.xhtml

Information about subscriptions to JNM can be found at:
http://jnm.snmjournals.org/site/subscriptions/online.xhtml

SNMMI | SOCIETY OF NUCLEAR MEDICINE AND MOLECULAR IMAGING